English

Performance of Ultra-Wide Band in Wireless Body Area Network (UWB-WBAN) System Over Additive White Gaussian Noise (AWGN) Channel

Mohanad Abdulhamid Al-hikma University, Iraq, email: moh1hamid@yahoo.com

Date of Receipt: August 13, 2023 | Approval date: July 25 , 2024

Abstract

The major constraints in the design of Wireless Body Area Network (WBAN) can be attributed to the battery autonomy, need for high data rate services and low interference from the devices operating within the industrial, scientific and medical (ISM) bands. ***Objective:*** *To meet the demand for high data rate services and low power spectral density to avoid ISM band interference, an ultra-wide band (UWB) system-based technology has been proposed.* ***Methodology:*** *This paper focuses on the design and demonstration of an UWB modem to be used in the WBAN applications and the evaluation of its performance in a near-real world scenarios affected by Additive White Gaussian Noise (AWGN) interference. The modem is tested with different values of signal to noise ratio (SNR).* ***Results:*** *Results show that the performance of the modem degrades as the value of SNR decreases.* ***Conclusion:*** *In conclusion, the modem simulation showed that it can achieve an error free transmission at a lower power spectral density and at a very high data rate.*

Key-words: Wireless Technology; Biomedical Technology; Telemedicine; Telemonitoring.

Resumen

Rendimiento de UWB-WBAN sobre el canal AWGN

Las principales limitaciones en el diseño de la Red de Área Corporal Inalámbrica (WBAN) se pueden atribuir a la duración de la batería, la necesidad de servicios de alta velocidad de datos y la baja interferencia de los dispositivos que operan en las bandas Industrial, Científica y Médica (ISM). ***Objetivo:*** *Para satisfacer la demanda de servicios de alta velocidad de datos y baja densidad espectral de potencia para evitar interferencias en la banda ISM, se propuso una tecnología basada en Banda Ultraancha (UWB).* ***Metodología:*** *Este artículo se centra en el diseño y la demostración de un módem UWB para ser utilizado en aplicaciones WBAN y la evaluación de su rendimiento en escenarios del mundo casi real afectados por la interferencia del Ruido Blanco Gaussiano Aditivo (AWGN). El módem se prueba con diferentes valores de Relación Señal-Ruido (SNR).* ***Resultados:*** *Los resultados muestran que el rendimiento del módem disminuye a medida que disminuye el valor SNR.* ***Discusión****: A partir de los resultados obtenidos, los gráficos de dispersión del tiempo y los diagramas de ojo muestran cuánto hay de interferencia de ruído.* ***Conclusión:*** *En conclusión, la simulación del módem mostró que es posible lograr una transmisión sin errores con una densidad espectral de potencia más baja y una velocidad de datos muy alta.*

Palabras clave: Tecnología inalámbrica; Tecnología Biomédica; Salud conectada; Telemonitoreo.

Resumo

Desempenho de UWB-WBAN sobre o canal AWGN.

As principais restrições no projeto de Rede Sem Fio de Área Corporal (WBAN) podem ser atribuídas à autonomia da bateria, à necessidade de serviços de alta taxa de dados e à baixa interferência dos dispositivos operando nas bandas Industriais, Científicas e Médicas (ISM). ***Objetivo:*** *Para atender à demanda por serviços de alta taxa de dados e densidade espectral de baixa potência para evitar interferência na banda ISM, foi proposta uma tecnologia baseada em Banda UltraLarga (UWB).* ***Metodologia:*** *Este artigo concentra-se no projeto e demonstração de um modem UWB para ser usado em aplicações WBAN e na avaliação de seu desempenho em cenários do mundo quase real afetados pela interferência de Ruído Gaussiano Branco Aditivo (AWGN). O modem é testado com diferentes valores de Relação Sinal-Ruído (SNR).* ***Resultados****: Os resultados mostram que o desempenho do modem diminui à medida que o valor do SNR diminui.* ***Discussão****: A partir dos resultados obtidos, os gráficos de dispersão do tempo e os diagramas de olho mostram o quanto há de interferência de ruído.* ***Conclusão:*** *Em conclusão, a simulação do modem mostrou que é possível obter uma transmissão livre de erros com uma densidade espectral de potência mais baixa e com uma taxa de dados muito alta.*

Palabras-clave: Tecnologia sem fio; Tecnologia Biomédica; Salud conectada; Telemonitoramento.

INTRODUCTION

Body area network (BAN), also referred to as a wireless body area network (WBAN) or a body sensor network (BSN) or *a medical body area network* (MBAN), is a wireless network of wearable computing devices. BAN devices may be embedded inside the body, implants, may be surface-mounted on the body in a fixed position wearable technology or may be accompanied devices which humans can carry in different positions, in clothes pockets, by hand or in various bags. Whilst there is a trend towards the miniaturization of devices, in particular, networks consisting of several miniaturized body sensor units (BSUs) together with a single body central unit (BCU). Larger decimeter (tab and pad) sized smart devices, accompanied devices, still play an important role in terms of acting as a data hub, data gateway and providing a user interface to view and manage BAN applications, in-situ.

The development of WBAN technology started around 1995 around the idea of using wireless personal area network (WPAN) technologies to implement communications on, near, and around the human body. About six years later, the term "BAN" came to refer to systems where communication is entirely within, on, and in the immediate proximity of a human body. A WBAN system can use WPAN wireless technologies as gateways to reach longer ranges. Through gateway devices, it is possible to connect the wearable devices on the human body to the internet. This way, medical professionals can access patient data online using the internet independent of the patient location.

A typical WBAN requires vital sign monitoring sensors, motion detectors (through accelerometers) to help identify the location of the monitored individual and some form of communication, to transmit vital sign and motion readings to medical practitioners or care givers. A typical body area network kit will consist of sensors, a processor, a transceiver (modem) and a battery. Initial applications of WBANs are expected to appear primarily in the healthcare domain, especially for continuous monitoring and logging vital parameters of patients suffering from chronic diseases. Other applications of this technology include sports, military, or security[1,2,3].

Because of the rather simple hardware realizations and the energy efficiency, ultra-wideband (UWB) communication has become one promising technology for the use in WBAN. UWB technology provides the high rate of data transmission due to its relatively large bandwidth of transmission. UWB spans a frequency range of 3.1GHz to 10.6GHz with a transmission bandwidth of more than 20% of its center frequency i.e. more than 500MHz. Based on this transmission bandwidth, it can be seen that the white Gaussian channel capacity of a UWB system is large for a given SNR according to Hartley Shannon law. Some works related to the use of UWB system in WBAN applications are found in some studies[4,5,6,7].

Therefore, based on the above, the objective of this article is to propose a technology based on ultra-wideband (UWB) systems that meets the demand for high data rate and low power spectral density services to avoid interference in the ISM band.

METHOD

Since the WBAN sensors have an integrated signal processing chips, the input to the transceiver is in digital form hence no need to include source coding as part of the transceiver design. The physical UWB transceiver design simulation which is done in Matlab simulink includes:

1. Random binary generator
2. Concatenated codes
3. QPSK modulator/ demodulator
4. OFDM transceiver.

Random binary generator

The Bernoulli binary generator is used to generate random binary digits using the Bernoulli distribution. It produces a zero bit (0) with a probability of *p* and a one bit (1) with probability of *1-p*.

In this case an equiprobable situation is simulated where both ‘0’ and ‘1’ are produced with a probability of 0.5. The output of this generator is frame based having 256 bits per frame at a sampling rate of 1/528MHz.

Concatenated codes

In wireless communications, burst errors occur due to the reflection of the symbols on large surfaces e.g. buildings, trees, hills etc. in addition, random errors also occur due to the thermal noise generated in the electronic circuitry. This calls for a coding scheme with a large codeword length. A serial concatenation of codes is the most used for power- limited systems.

In this case, a (48, 32, 8) Reed-Solomon(R-S) code (outer code) with symbols over GF (28) and a (2, 1) convolution code of constraint length 7 was used.

Reed Solomon coding/decoding

A (48, 32, 8) R-S code over GF (28) was obtained by code shortening scheme of puncturing (zero padding) as shown in Fig.1 in a matlab simulink model. This code corrects up to 8 symbol errors out of the 48 symbols.

Since R-S encoder is a non-binary coding scheme, the 256-bit frame from the Bernoulli generator is converted to integers using bit to integer converter of 8, resulting into 32 bytes which is the input sequence to the R-S encoder subsystem.

Figure 1. R-S encoder

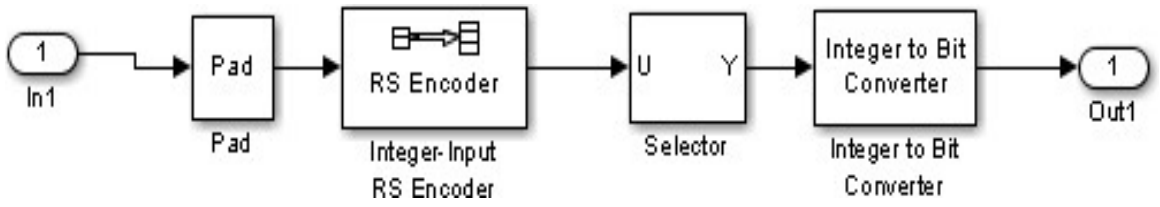

The 32-byte sequence is zero padded to 239 message bytes which is then fed to the integer input R-S encoder. This block adds 16 parity check bytes to give 255 codeword length. Since we are interested in the 48 code words, the zero padded 255 code words is passed through a selector to give the 48 codewords hence a (48, 32, 8) R-S code achieved from the (255, 239,8) R-S code. The 48 bytes is converted back to binary to give 384 bits which is passed through to the convolution encoder.

In the decoder shown in Fig.2, the 384 bits is converted to bytes, zero padded to and fed to the decoder which decodes the message i.e. corrects any error introduced during the transmission and removes the parity check bits. The zero padded 239 message digits from the decoder is passed through a selector to obtain the 32 original message digits which are then converted back to binary.

Fig.2 R-S decoder

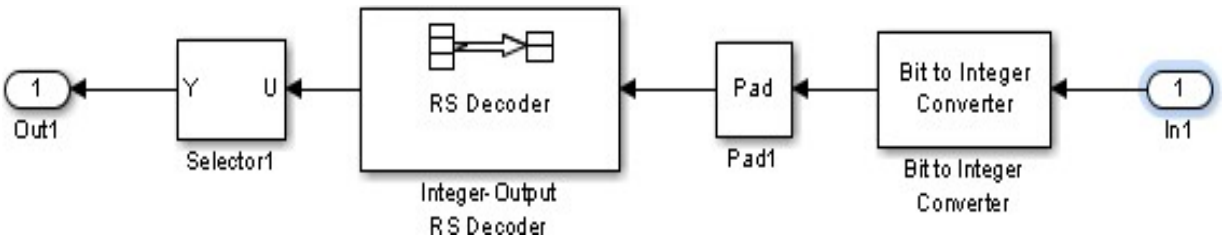

Convolution coding/ Viterbi decoding

This convolution code has an information rate of ½ and constraint length of 7. It uses the polytrellis (7, [171 133]) function to create a trellis using the constraint length, code generator (octal) and feedback connection (octal). As can be seen from the Fig.3,

Output [a, b] = input input [x_1 , x_2]]

Where x_1,=(1111001)= $(171)_8$

x_2=(1011011)=$(133)_8$

ISSN: 2175_2990 | Latin Am J telehealth, Belo Horizonte, 2022; 9 (3): 327 - 339

Fig.3 Polytrellis(7[171,133]) structure

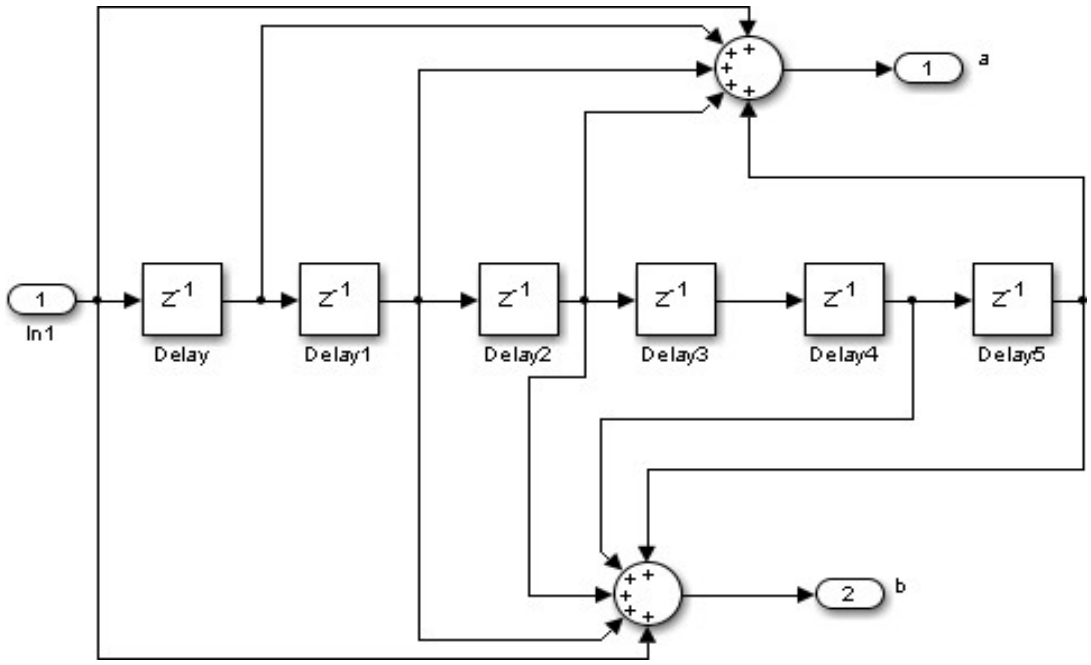

The Viterbi decoder also uses the same polytrellis function while decoding the information transmitted. Since the information rate is ½, this implies that for every one bit, two codewords are produced hence the output of the convolution encoder is 768 bits. The Viterbi decoder, detects and corrects the random errors and removes the parity check bits hence its output is 384 bits.

QPSK modulator /demodulator

The quadrature phase shift keying (QPSK) modulator maps the binary digits from the information sequence into discrete phases of the carrier as shown in Fig.4.

Fig.4 QPSK constellation mapping

The 768 message bits are converted to integers and then fed into the QPSK modulator which maps the 384 integers to complex 384 integers. QPSK demodulator performs inverse operation of QPSK modulator.

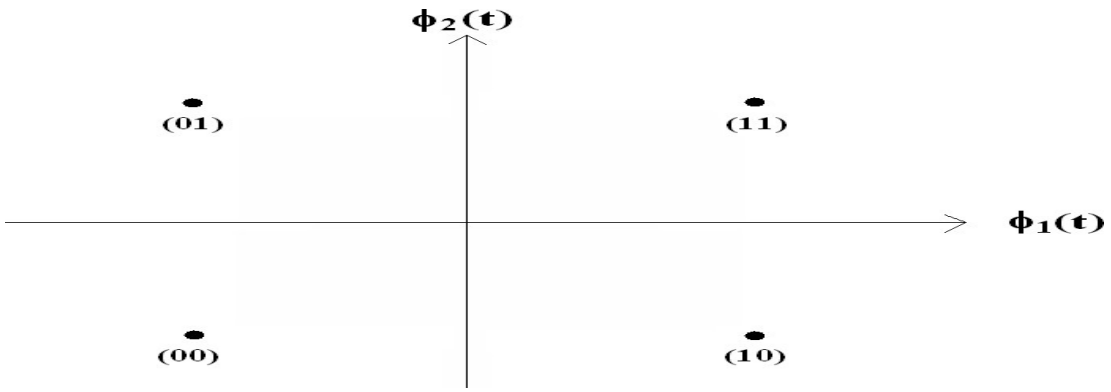

ISSN: 2175_2990 | Latin Am J telehealth, Belo Horizonte, 2022; 9 (3): 327 - 339

OFDM transceiver

Orthogonal frequency division multiplexing (OFDM) symbol consist of the data carriers, guard subcarriers and the cyclic prefix, with time durations as shown in Fig.5. In this design, 128 subcarriers are used, with 96 being data carriers, 12 pilots and 20 nulls for guard. A cyclic prefix of 32 subcarriers is appended. The 384 complex integers are rearranged to form 96x4 array matrix.

The matrix is regrouped as: {1,[2:10],[11:19],[20:28],[29:37],[38:46],[47:50],[51:54],[55:62],[63:70],[71:78],[79:86],[87:96]} to allow the insertion of the pilots. The pilots are inserted at the positions (2, 12, 22, 32, 42, 52, 61, 70, 79, 88, 97, 108).

The guards are then inserted at the beginning and end of the data carriers. The symbol is then passed through the inverse fast Fourier transform (IFFT) to create the orthogonal signals. A cyclic prefix is appended by rearranging and reordering the sequence as [97:128 1:128]. This command repeats the last 32 carriers at the beginning of the OFDM symbol.

The OFDM symbol is then power scaled and transmitted via the AWGN channel. The OFDM transmitter is designed as shown in Fig.6

Fig.5 OFDM symbol

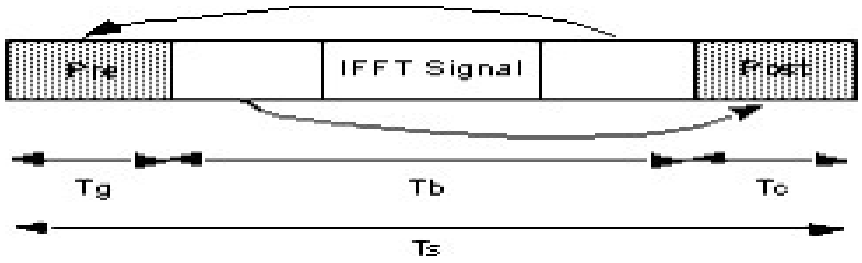

Fig.6 OFDM transmitter

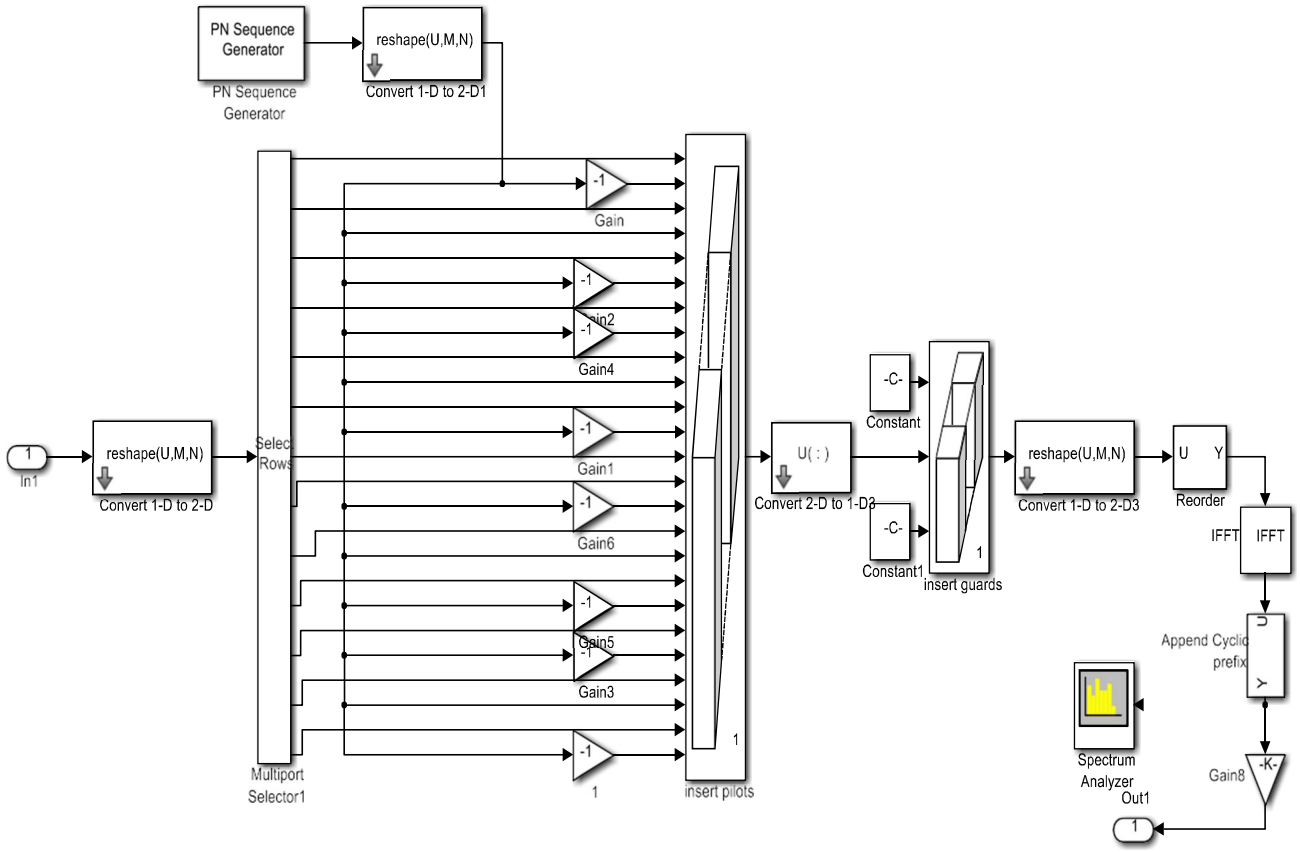

Fig.7 OFDM receiver

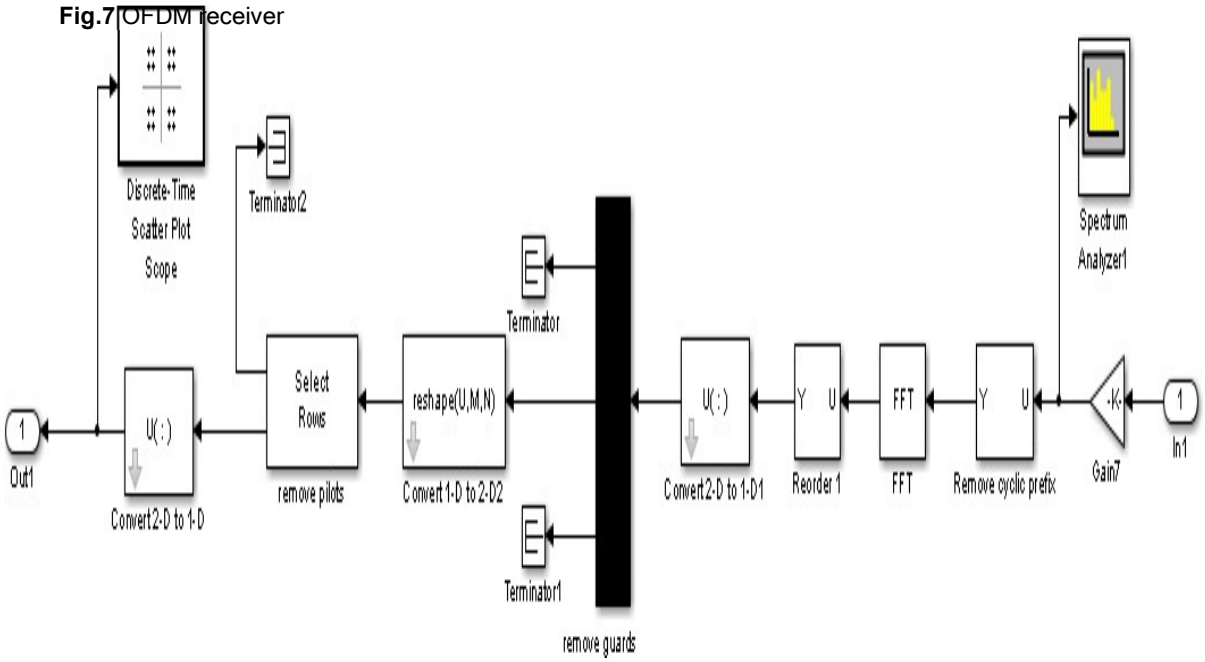

At the OFDM receiver shown in Fig.7, the received symbol is down scaled, and the cyclic prefix is removed by selecting the message portion. The received message is then transformed by fast Fourier transform (FTT) to remove the orthogonality. The guards are then removed and subsequently the pilots. The remaining data stream is then rearranged back to the 384 constellation points and then demodulated using QPSK demodulator.

The channel

The type of channel used here is AWGN channel. This channel adds white Gaussian noise to the input signal. The SNRs of 10dB, and 20dB are simulated and results displayed.

Overall design diagram

The overall design is shown in Fig.8

Fig.8 Overall Design

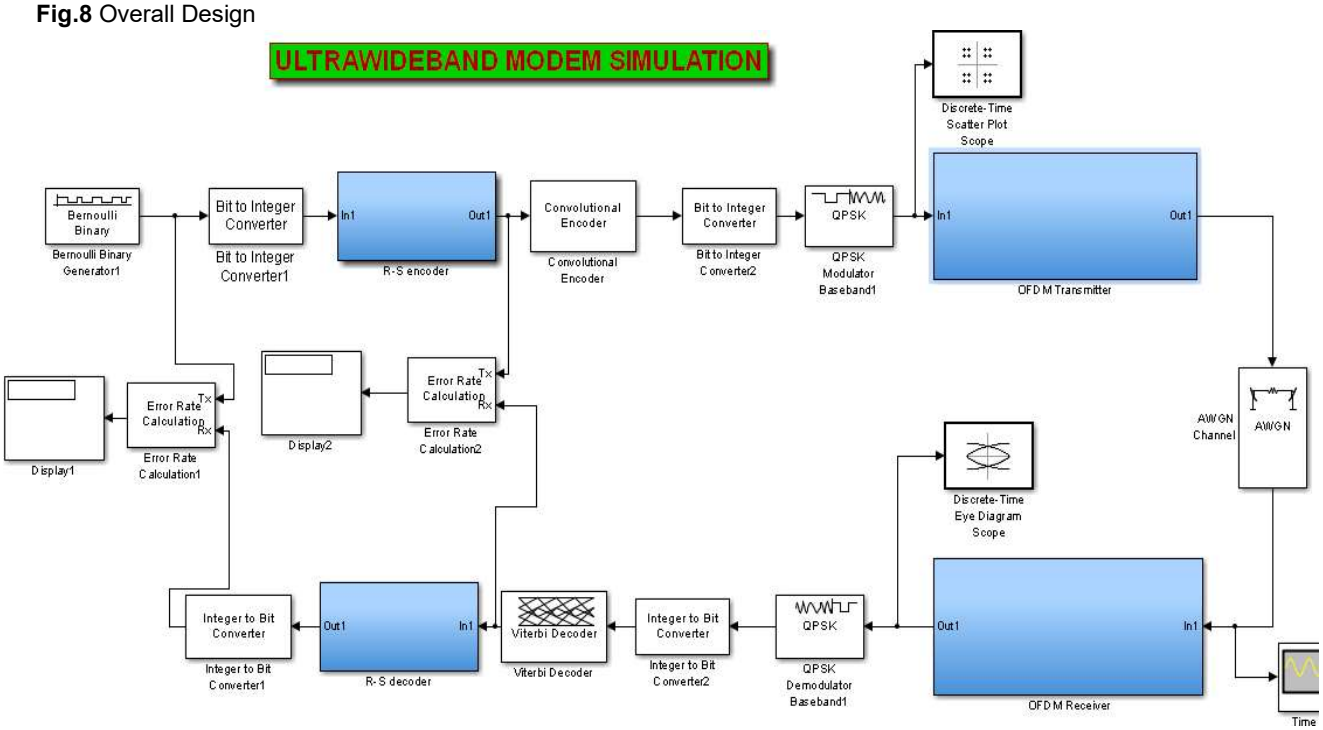

RESULTS

Results for SNR=10dB

Fig.9 to Fig.12 show the transmitted signal, received signal, error rate calculation, and signal spectrum respectively for SNR=10dB. It can be seen from Fig.11 that the error rate calculation is 0.4102. By comparing between transmitted signal (Fig.9) and received signal (Fig.10), it can be concluded that there is some difference between them due to noise effect.

Fig.9 Transmitted signal

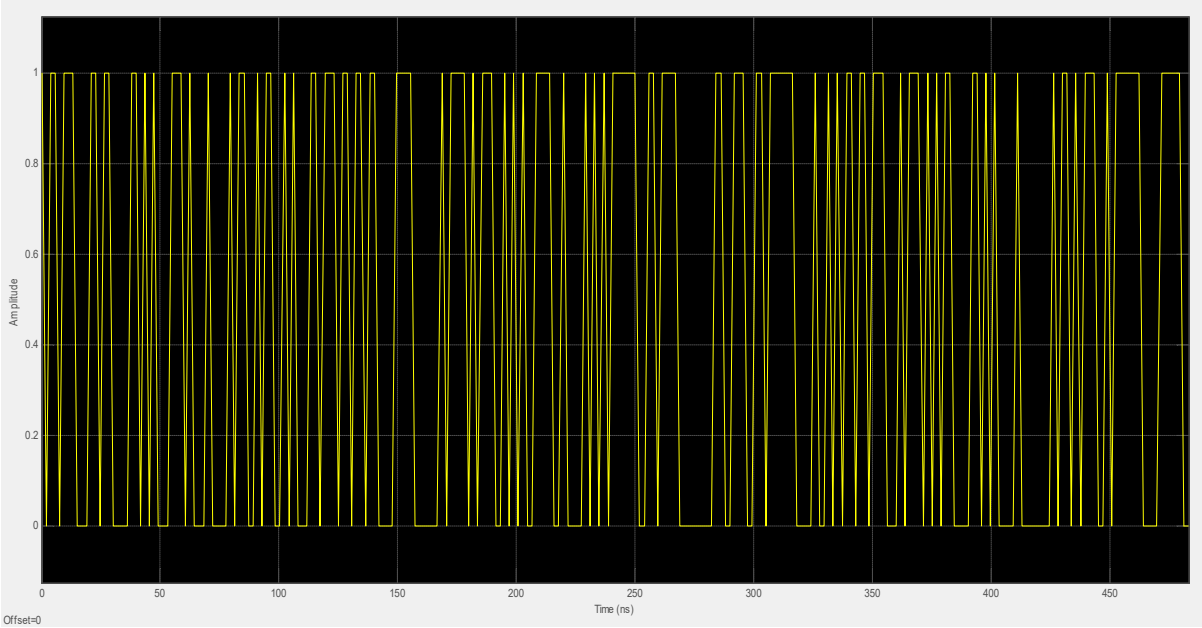

Fig.10 Received signal

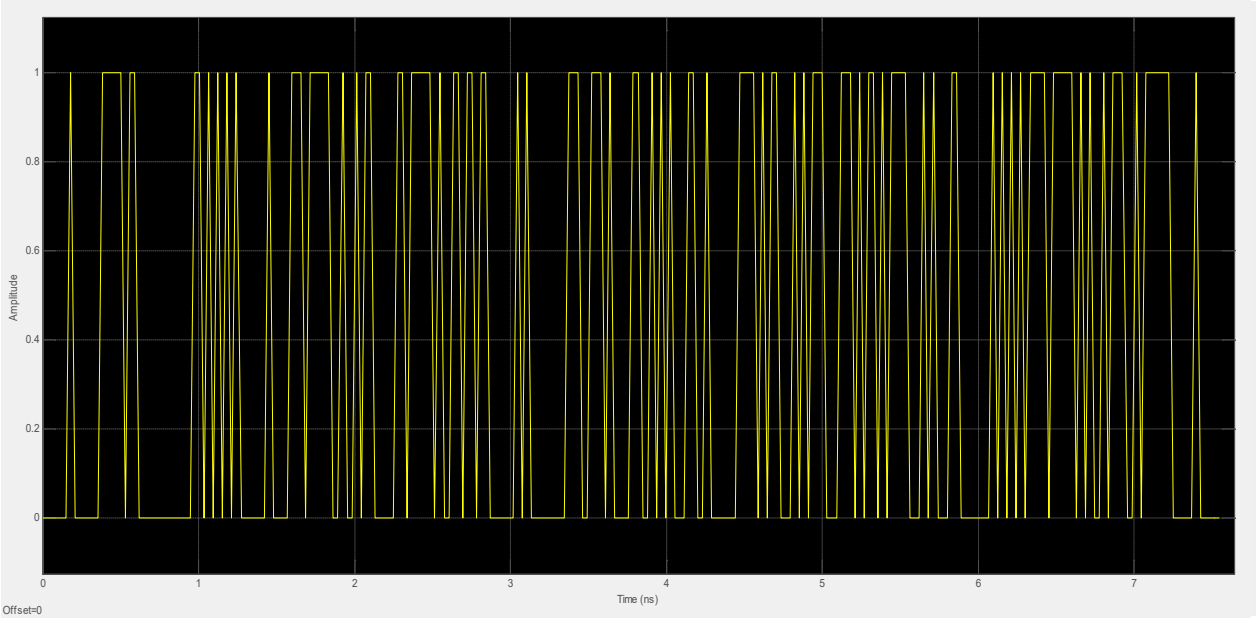

Fig.11 Error rate calculation

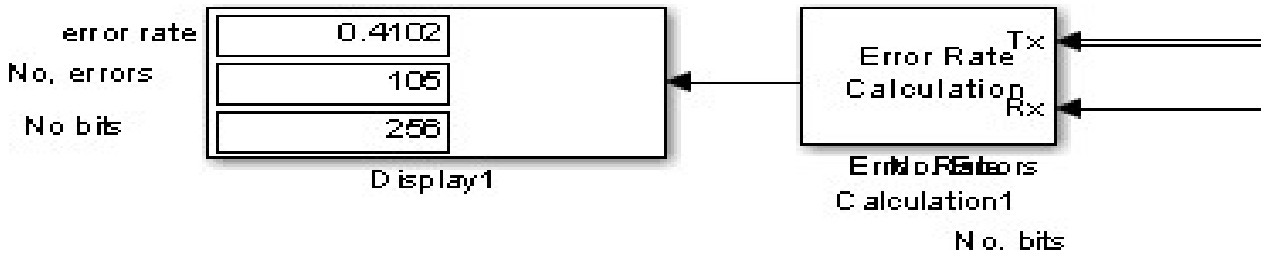

Fig.12 Signal spectrum

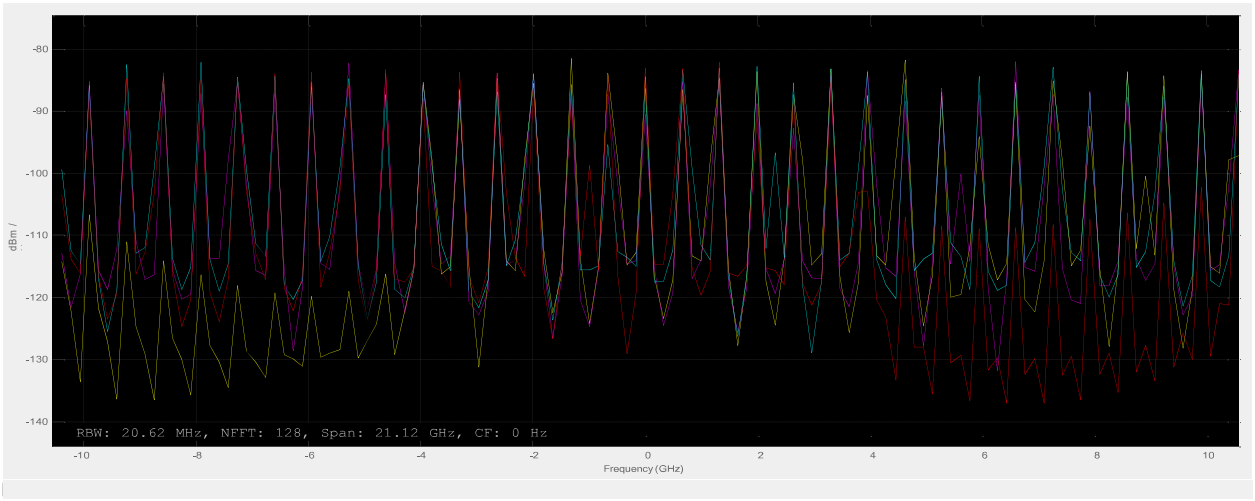

Fig.13 Eye diagram

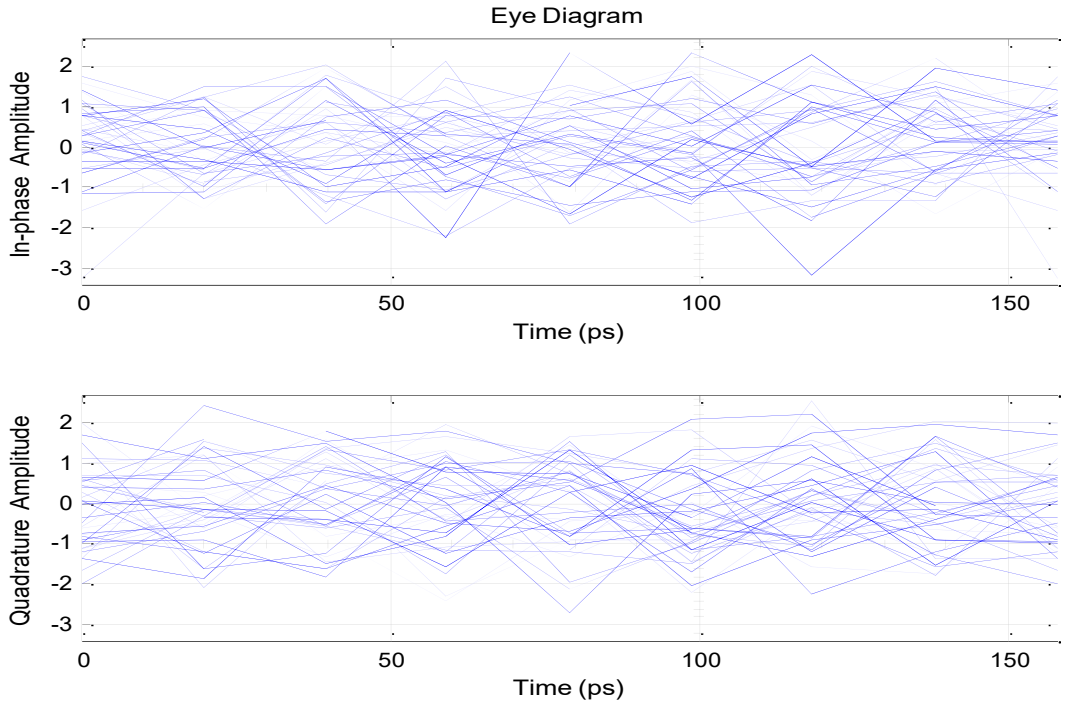

ISSN: 2175_2990 | Latin Am J telehealth, Belo Horizonte, 2022; 9 (3): 327 - 339

Fig.14 Time scatter plot

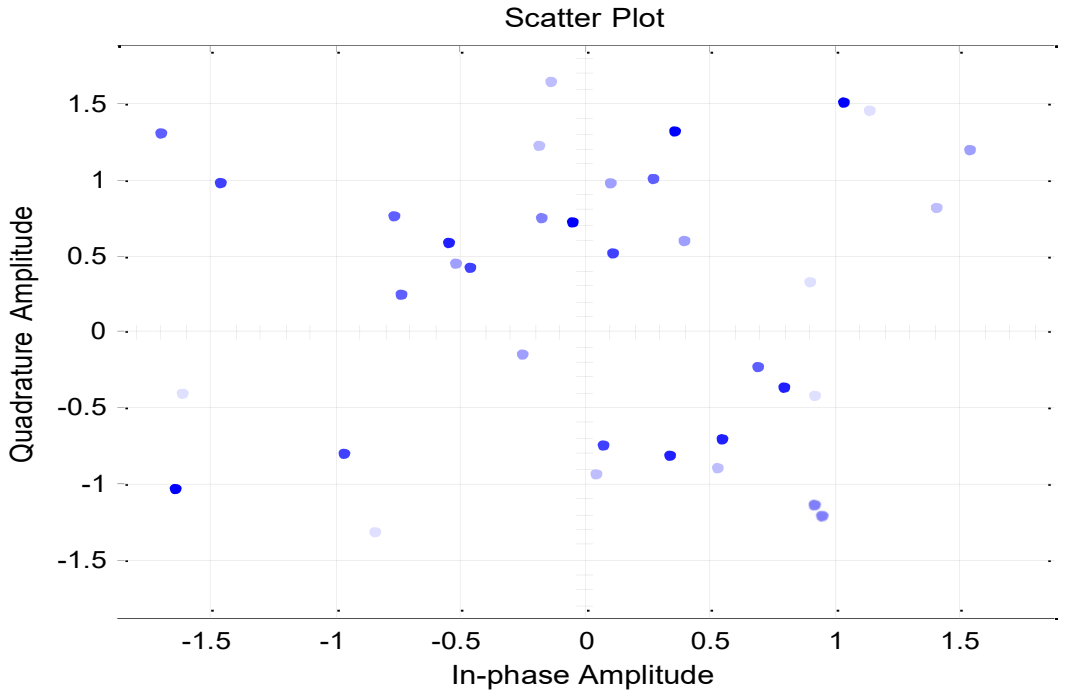

Results for SNR=20dB

Fig.15 to Fig.18 show the transmitted signal, received signal, error rate calculation, and signal spectrum respectively for SNR=20dB. From Fig.17, the error rate calculation is zero due to high SNR. By comparing between transmitted signal and received signal, it can be concluded that the two signals are identical due to error free

Fig.15 Transmitted signal

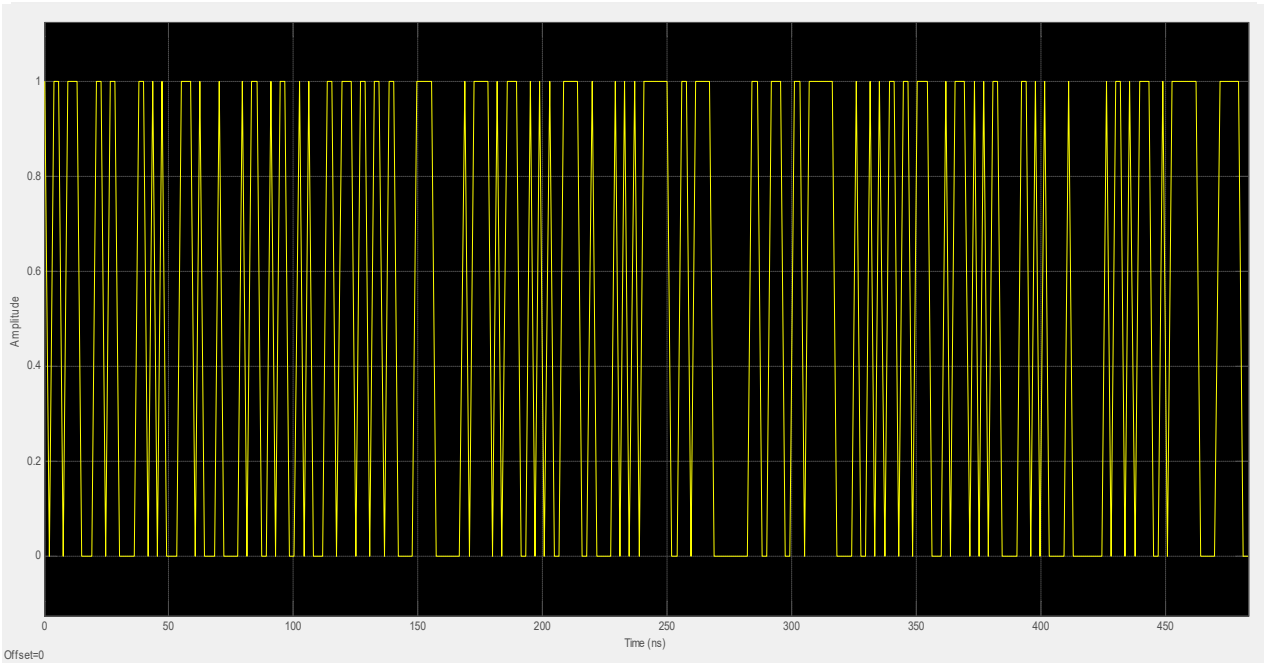

Fig.16 Received signal

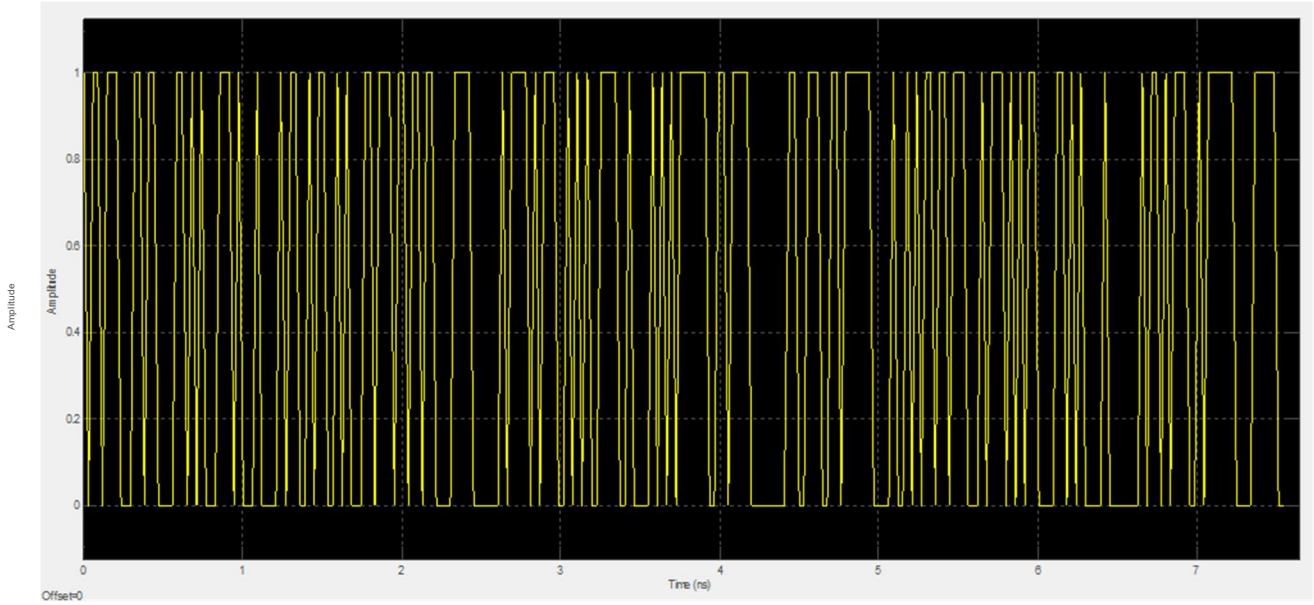

Fig.17 Error rate calculation

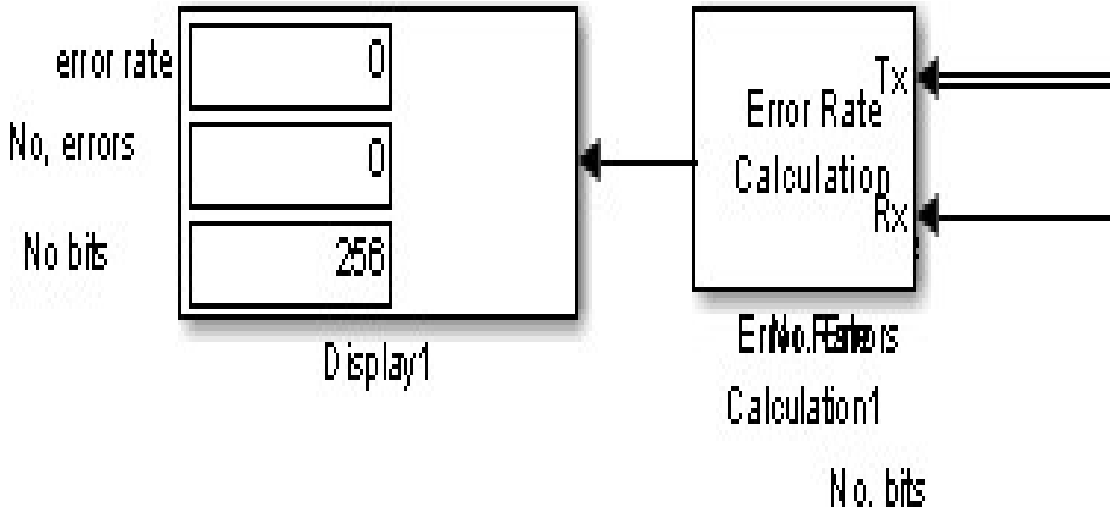

ISSN: 2175_2990 | Latin Am J telehealth, Belo Horizonte, 2022; 9 (3): 327 - 339

Fig.18 Signal spectrum

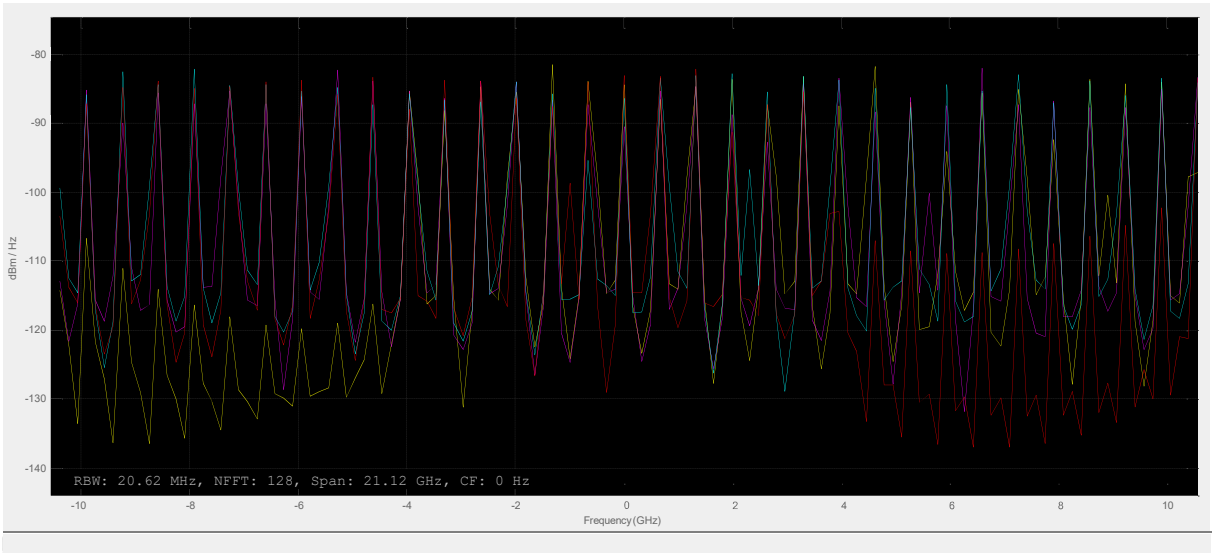

Fig.19 and Fig.20 show the eye diagram and time scatter plot for SNR=20dB. It seems from the two figures that the distortion almost disappear as noise effect vanished.

Fig.19 Eye diagram

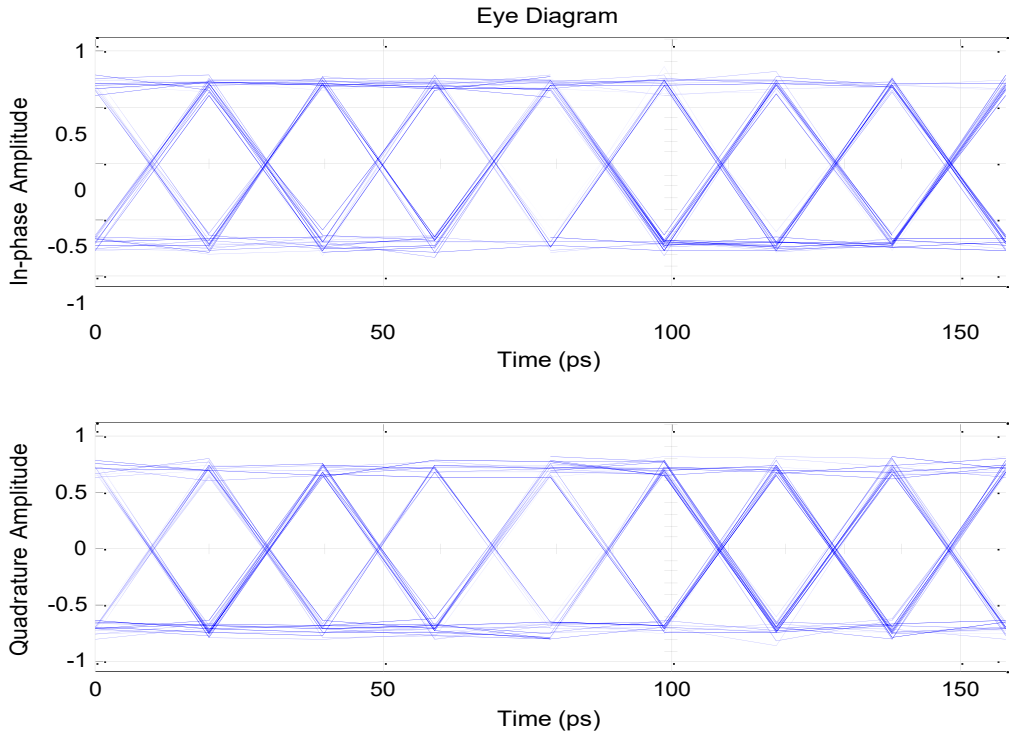

Fig.20 Time scatter plot

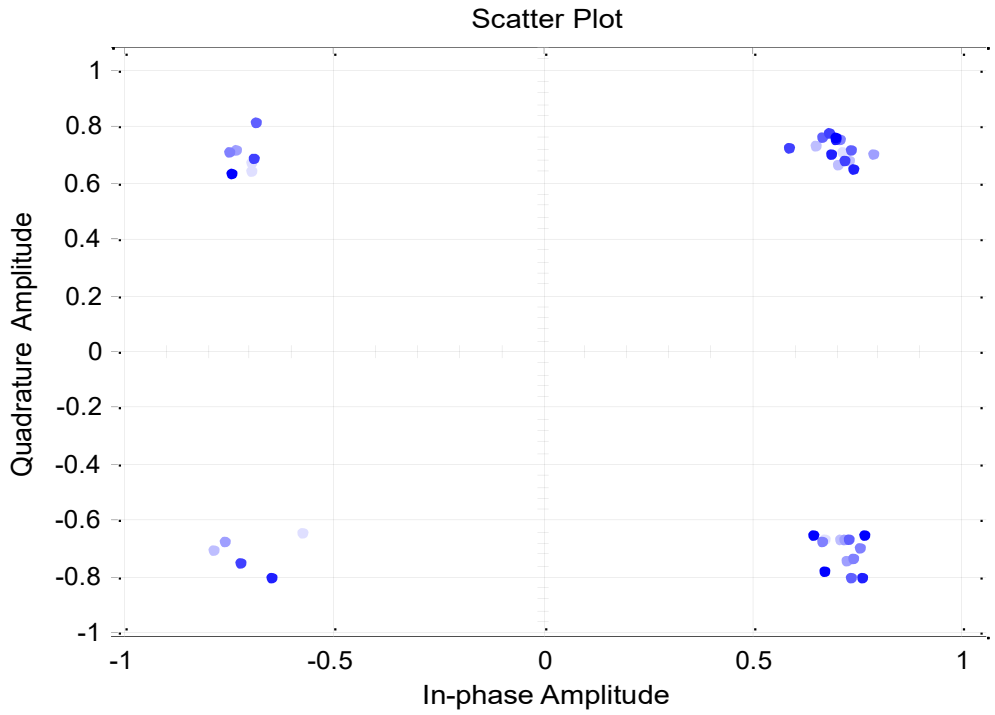

DISCUSSION

From the results obtained, the time scatter plots, and the eye diagrams show how much is noise interference. The wider the eye the lower the noise interference. This is further proved by looking at the scatter plots, if the plots are randomly distributed, then the noise power is higher than the signal power. This analysis plus the results shows that for a given transmission bandwidth, the system performance improves as the SNR increases. The error calculations done further proves that indeed as the SNR increases, an error free transmission is possible.

CONCLUSIONS

This paper studied both the UWB wireless communication systems and WBAN applications and then designed and demonstrated a modem to be used in those applications. The modem simulation showed that it can achieve an error free transmission at a lower power spectral density and at a very high data rate.

REFERENCES

1. G. Crosby, et. al. ,"Wireless body area networks for healthcare: A survey", International Journal of Ad hoc, Sensor & Ubiquitous Computing, Vol.3, No.3, 2012.

2. M. Samaneh, et. al.," Wireless body area networks: A survey", IEEE Communications Surveys and Tutorials,Vol.16, Issue 3, 2014.

3. G. Ragesh, and K. Baskaran ,"An overview of applications, standards and challenges in futuristic wireless body area networks", International Journal of Computer Science Issues,Vol.9, Issue 1, No.2, 2012.

4. M. Abdulhamid, and O. Ben Sewe, " On the performance of UWB-WBAN modem", Scientific Bulletin of Electrical Engineering Faculty, Vol.18, Issue 2, 2018.

5. E. Hamza, and R. Majeed,"MAC Protocol for UWB wireless body area networks", American Scientific Research Journal for Engineering, Technology, and Sciences, Vol.38,No.1, 2017.

6. M. Ali," Low power FM-UWB transmitter for wireless body area networks", Ph.D. thesis, Electronics Research Institute, Egypt, 2017.

7. O. Ben Sewe,"Ultra-wideband modem for wireless body area network applications", Graduation Project, Nairobi University, Kenya, 2014.

Indication of responsibility: I Declare that all author have participated in the construction and elaboration of the work and Detail the responsibilities of each author in carrying out the article]

Financing: There is no funding.

Conflict of interest: The author declare that there are no conflicts of interest regarding thisresearch, authorship, or publication of this article.

How to cite this article: Abdulhamid M. Performance of Ultra-Wide Band in Wireless Body Area Network (UWB-WBAN) System Over Additive White Gaussian Noise (AWGN) Channel. Latin American Journal of Telehealth Latin Am J telehealth, Belo Horizonte, 2022; 9 (3): 327 – 339. ISSN: 2175_2990.